# Intratumoral plasmid IL-12 expands CD8+ T cells and induces a clinically validated CXCR3 signature in triple-negative breast cancer

Erika J. Crosby[1], Hiroshi Nagata[1], Melinda L. Telli[2], Chaitanya R. Acharya[1], Irene Wapnir[3], Kaitlin Zablotsky[3], Bernard A. Fox[4], Carlo B. Bifulco[4], Shawn M. Jensen[4], Carmen Ballesteros-Merino[4], Erica Browning[5], Reneta Hermiz[5], Lauren Svenson[5], Donna Bannavon[5], Kellie Malloy Foerter[5], David A. Canton[5], Chris G. Twitty[5], Takuya Osada[1], H. Kim Lyerly[1,6,7]

[1]Duke University Medical Center, Department of Surgery, Durham, NC; [2,3]Stanford University School of Medicine, Departments of Medicine[2] & Surgery[3], Stanford, CA; [4]Earle A. Chiles Research Institute, Providence Portland Medical Center, Portland, OR; [5]OncoSec Medical Incorporated, San Diego, CA; [6,7]Duke University Medical Center, Departments of Pathology[6] and Immunology[7]

Duke Surgery
Duke University School of Medicine

## Background

- Sustained disease control and prolonged survival in patients with triple-negative breast cancer (TNBC) is uncommon, highlighting the need for improved immune-based strategies particularly in poorly immunogenic tumors
- Interleukin-12 (IL-12) is involved in the generation of adaptive immune responses, an inflammatory tumor microenvironment and is critical in eliciting a productive anti-tumor immune response[1,2]
- Intratumoral injection of plasmid IL-12 (tavokinogene telseplasmid; TAVO) followed by electroporation (EP) (IT-TAVO-EP, collectively designated TAVO) is a gene therapy approach that drives local and immunologically relevant exposure of IL-12 with minimal systemic immune-related toxicity[3-5]
- CXCL9/10/11/CXCR3 axis regulates the migration, differentiation, and activation of both innate and adaptive immune cells[6]

## Methods

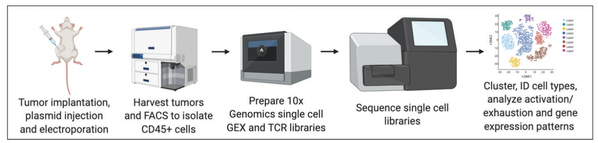


- Murine TNBC (4T1) cells were orthotopically implanted into mice and allowed to establish prior to treatment with TAVO or control plasmid
- On Days 0, 4 and 7, the mice underwent IT administration of plasmid, followed by in vivo electroporation
- Tumors were digested and CD45+ cells sorted for single cell RNA sequencing
- Analyses performed include cell type identification, gene signature definition, receptor-ligand interactions, and pathway analysis
- Gene expression and gene signatures identified were applied to METABRIC database
- IHC and NanoString analysis of matched pre- and post-TAVO tumor biopsies from OMS-I140 was performed to compare gene signatures. Data from this study reported previously.[7]

### References

1. Lyerly HK, Osada T, Hartman ZC. *Clin Cancer Res*. 2019;25:9-11.
2. Osada T, et al. *Cancer Immunol Immunother*. 2012;61:1941-1951.
3. Algazi A. et al. *Ann Oncol*. 2020;31:532-540.
4. Algazi AP, et al. *Clin Cancer Res*. 2020. doi:10.1158/1078-0432.Ccr-19-2217.
5. Daud AI, et al. *J Clin Oncol*. 2008;26:5896-5903.
6. Metzemaekers M, Vanheule V, Janssens R, Struyf S, Proost P. *Front Immunol*. 2018;8. doi:10.3389/fimmu.2017.01970.
7. Telli ML, Wapnir I, Devitt B, et al. San Antonio Breast Cancer Symposium 2019. Abstract P3-09-04.

**Abbreviations:**
BC, breast cancer; PD-1, programmed cell death receptor 1; PD-L1, programmed cell death ligand 1; EOS, end of study; DC, dendritic cell; TAVO, tavokinogene teleplasmid; IL-12, interleukin-12; METABRIC, Molecular Taxonomy of Breast Cancer International Consortium; TIL, tumor infiltrating lymphocytes; IHC, immunohistochemistry; TNBC, triple-negative breast cancer; TCR, T cell receptor

## Results

### Figure 1. TAVO treatment inhibits tumor growth and enhances immune cell infiltration

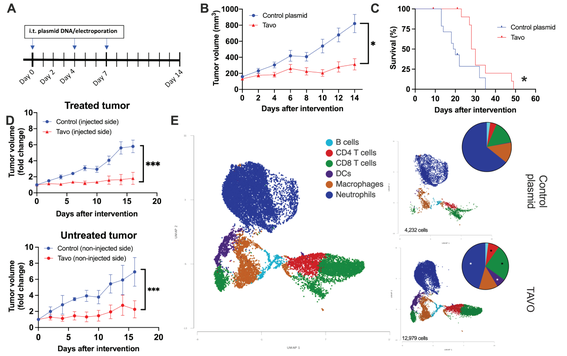


**A.** Treatment Schedule. When the tumor size reached 6-7 mm in diameter, mice were randomized into two groups (day 0) and received intratumoral injections of plasmid followed by in vivo electroporation as indicated. **B.** Growth inhibition of 4T1 tumors by intratumoral TAVO administration. (TAVO n=13, control n=14). **C.** Survival of mice in (B) **D.** Abscopal effect of intratumoral TAVO administration. Tumor volumes were normalized to size at treatment initiation (on day 0 Upper graph: treated tumors. Bottom graph: untreated tumors. **E.** UMAP plot of CD45+ cells sorted from tumors and classified into cell types for all samples or divided by treatment group including proportional analysis of each cell type in each treatment group (inset). All error bars represent mean ± SEM *$p$<0.05; ***$p$<0.001.

### Figure 2. Expansion and activation of T cell in TAVO treated tumors

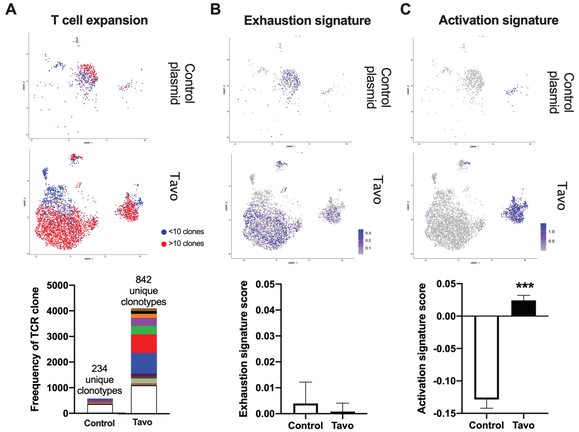


**A.** (top) UMAP showing reclustering of all TCR+ cells from Figure 1E colored by expansion of clones (<10=blue; >10=red) (bottom) quantification of the frequency of each clone with the top 50 clones for each treatment shown in colored bars. **B.** (top) UMAP from A. colored by 50 gene exhaustion signature score. (bottom) Quantification of exhaustion signature score across all T cells in each treatment. **C.** (top) UMAP from A. colored by 50 gene activation signature score. (bottom) Quantification of activation signature score across all T cells in each treatment. All error bars represent mean ± SEM ***$p$<0.001.

### Figure 3. TAVO treatment induces expression of a CXCR3 signature and upregulates PD-1/PD-L1 pathway

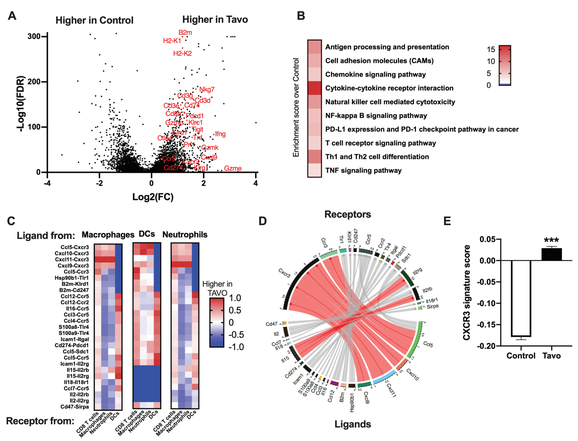


**A.** Volcano plot of differentially expressed genes in TAVO or control treated cells. Genes shown have FDR<0.05 and fold change>|2|. **B.** Selected KEGG pathways that are significantly enriched in TAVO treated tumors. **C.** Interactome scores for each indicated cell type comparing receptor-ligand interaction in control and TAVO treated cells. DC= dendritic cell **D.** Circos plot depicting receptor-ligand interactions between receptors on CD8+ T cells and ligands on macrophages. Connections shown in red represent the top 10% of interactions between these cell types. **E.** 50 gene CXCR3 signature scores quantified across all cells. All error bars represent mean ± SEM ***$p$<0.001.

### Figure 4. CXCR3 signature expression is correlated with improved survival in METABRIC data set.

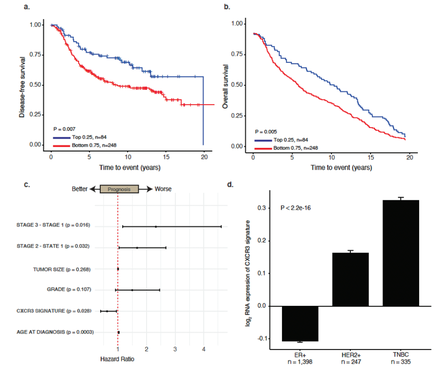


**A.** Kaplan-Meier survival curves for disease-free survival and **B.** Overall survival from n=335 primary TNBC patients. Log-rank p-values are shown. **C.** Hazard ratios and confidence intervals derived from Cox regression survival analysis for disease-free survival in multivariable analyses. **D.** Boxplot showing relative enrichment of CXCR3 signature in TNBC compared to other BC subtypes.

### Figure 5. Clinical data demonstrates that TAVO induces an increase in CXCR3 gene signature that is significantly associated with TIL infiltration

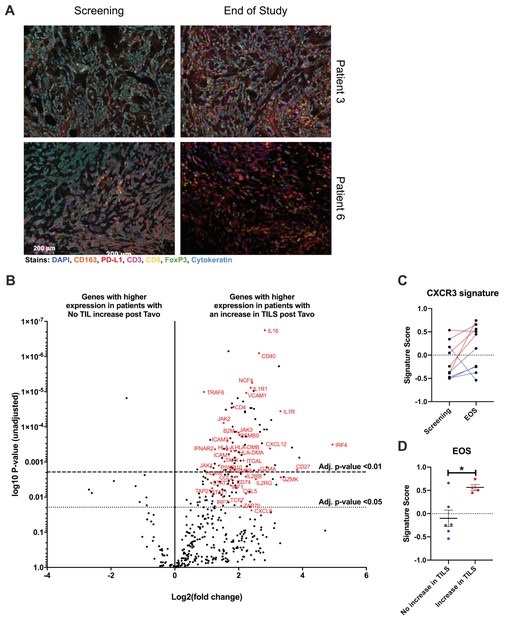


**A.** Representative multispectral IHC images from indicated patients at screening and end of study (EOS) in OMS-I140. Scale bar applies to all images. **B.** Volcano plot of differentially expressed genes from NanoString assay in all 10 patients with or without an increase in CD8+ TIL as measured by IHC. Adjusted p-values of <0.01 and <0.05 are indicated by dashed lines. **C.** Paired signature scores for adapted CXCR3 gene signature from preclinical assay at screening and EOS. **D.** CXCR3 signature scores at EOS split by patients with no increase in TIL and an increase in TIL. All error bars represent mean ± SEM *$p$<0.05.

## Summary & Conclusions

- TAVO treatment overcomes an immunologically 'cold' tumor microenvironment by increasing antigen presentation, expanding and activating T cells, and minimizing the infiltration of potentially suppressive granulocytic cells
- There is an increase in expression of PD-1/PD-L1 and the CXCL9/10/11/CXCR3 pathways, including a CXCR3 associated 50-gene signature that is enhanced in patients with an increased infiltration of CD8 T cells
- Expression of CXCR3 gene signature is prognostic in METABRIC samples for TNBC